

# NOMA-enabled Cooperative V2V Communications with Fixed-Gain AF Relaying

Semiha Koşu and Serdar Özgür Ata

**Abstract**—By virtue of its improving bandwidth efficiency along with user fairness, non-orthogonal multiple access (NOMA) technique is considered a promising method for next-generation wireless communication systems. Since fading effect of wireless channels in vehicle-to-vehicle (V2V) communication systems are more severe than those in traditional systems, in this study, we employ the power-domain downlink NOMA technique in cooperative V2V communication systems to enhance data transmission capacity and network efficiency. In the proposed system, the base station communicates with two vehicular nodes, namely near and far users, through a relay vehicle employing the fixed-gain amplify-and-forward scheme. In real-life scenarios, the relay and the users move in high velocities; hence, the corresponding fading channels between these nodes are exposed as having double-Rayleigh fading characteristic in which the fading coefficient of a wireless channel is modeled as the product of two Rayleigh distributed random variables. To analyze the system performance, we first investigate the outage probability and derive its exact closed-form expressions for the near and far users. Then, we make the exact ergodic capacity analysis and obtain the closed-form solution for the near user. Furthermore, outage and ergodic performances of the NOMA-enabled system are compared to the simulation results of the traditional orthogonal multiple access approach. We also give analytic and numerical results to evaluate the performance of the proposed system and show the consistency of Monte-Carlo simulations with analytical derivations. It is observed that even with the small power allocation, both performances of the near user mostly outperform the far user.

**Index Terms**—Amplify-and-forward, cooperative communications, double Rayleigh, ergodic capacity, fixed-gain, non-orthogonal multiple access, outage probability, vehicular networks.

## I. INTRODUCTION

**I**N wireless communication systems, multiple access methods are used in order to allocate limited resources effectively to many users [1]. Well-known orthogonal multiple access (OMA) techniques used in current cellular communication systems, such as time division multiple access, frequency division multiple access or code division multiple access, cannot fulfill the higher spectral efficiency and enhanced user fairness requirements of 5G and beyond technologies. Recently, non-orthogonal multiple access (NOMA) has been proposed to be an outperforming multiple access technique which offers higher spectral efficiency in comparison with OMA techniques

by allowing multiple users to simultaneously transmit their signal with different power levels in the same resource block (i.e, frequency, time, code) [2]. In addition to enhanced spectrum usage efficiency, NOMA can ensure high fairness among multiple users through optimized power allocation schemes, in which users suffering poor channel conditions, namely weak/far users, receive their signals with a higher power while users experiencing better channel conditions, namely strong/near users, receive lower power information symbols. Hence, the strong users achieving high signal-to-interference-plus-noise ratio (SINR) will be able to decode their own signal by using successive interference cancellation (SIC) methods while the weak ones having low SINR may decode their own signals by treating the strong users' signals as interference.

Vehicle-to-vehicle (V2V) communications has attracted increasing interest as an important application area of 5G technology with the opportunities it offers such as in-vehicle internet access and autonomous driving, as well as intersection management and preventing densities by regulating the traffic flow, collision avoidance and rapid response to accidents, roadway reservation and increasing road safety [3]–[8]. Compared to cellular communication systems, the design of V2V communication systems has its own challenges. One of these is that the fading effect in wireless communication channels is worse compared to the fading effect encountered in cellular communication systems due to factors such as high speeds of vehicles, low vehicle-antenna heights, and high number of scattering obstacles [9]. Many studies in the literature have shown that the fading effect in V2V communication channels can be modeled as the product of several random variables. These types of channels are named cascaded fading channels. Again in these studies, it has been revealed by field measurements that a suitable channel model for modeling the V2V communication channels is the double Rayleigh fading channel model in which the fading gain of the wireless channel can be expressed as the product of two independent Rayleigh distributed random variables [9]–[12]. However, there are very few studies in the literature focusing on V2V communication systems over cascaded fading channels compared to studies on traditional cellular communication systems. This is mainly because the closed-form solutions for the performance analysis of these channels cannot be obtained most of the time due to intractable integrals resulting from special functions included in the cumulative distribution function (CDF) and probability density function (PDF) expressions of SINR.

**Semiha Koşu** is with the Department of Informatics Institute, Istanbul Technical University, 34469 Istanbul, TURKEY e-mail: kosu18@itu.edu.tr

**Serdar Özgür Ata** is with the Informatics and Information Security Research Center, TUBITAK-BILGEM, Kocaeli, TURKEY e-mail: serdar.ata@tubitak.gov.tr

Manuscript received Mar 21, 2022; accepted Dec 30, 2022. DOI: 10.17694/bajece.1090937

### A. Related Works

As an effective performance-enhancer technique, cooperative communications has been studied extensively over two decades. Amplify-and-forward (AF) and decode-and-forward (DF) relaying methods [1] were proposed to achieve better performance in many V2V communication scenarios where line-of-sight (LOS) is not available between source and destination nodes due to reasons such as vehicles with low-antenna heights in urban areas or communication through very long distances in rural areas. In the literature, cooperative V2V systems over cascaded fading channels are studied in [13]–[18]. In [13], outage probability and achievable diversity order are examined for DF relaying in V2V communication systems by applying the best relay selection scheme over cascaded Rayleigh fading channels. In [14], by using the moment generation function approach, higher-order moments of the signal-to-noise ratio (SNR), average symbol error probability, and ergodic capacity are derived for the bi-directional AF transmission system over cascaded Nakagami- $m$  channels. In [15], the probability of detection is investigated in an inter-vehicular cooperative cognitive radio system using the maximum ratio combining (MRC) diversity technique when the channels are exposed to cascaded Rayleigh fading. In [16], the minimized total error rate and the probability of detection are analyzed over mixture Gamma distributed fading channels for a cooperative spectrum sensing system employing different diversity combining techniques with multiple antenna nodes. In [17], the authors studied a cooperative V2V interference-limited communication system with DF relaying operating over double-Nakagami fading channels. Exact and asymptotic expressions for outage and average symbol error probabilities are obtained for the cases of best relay selection and threshold-based relay selection schemes. The outage performance of V2V networks employing full-duplex (FD) and half-duplex (HD) relaying schemes is investigated in [18] and the upper bounds for the outage probability are derived for AF and DF relaying over double Rayleigh fading channels.

In recent years, in order to fulfill robustness and reliability requirements of next generation technologies, NOMA and cooperative communication techniques are addressed together in system design [19]–[29]. In [19], asymptotic outage probability and ergodic sum-rate analyses are derived for a NOMA-inspired AF relaying system where the source and the relay simultaneously transmit two symbols in a message. Additionally, in [19], the authors propose a mixed MRC-SIC scheme for received superimposed signals at the destination. In [20], the authors applied the NOMA technique to an AF relaying system to maximize the achievable secrecy sum rate by jointly designing power allocation at the source and cooperative beam-forming at the relay, under achievable rate constraints at the weak users and transmit power constraints at the source and the relay. [21] investigates the performance of AF relaying scheme using NOMA, where two sources communicate with their corresponding destinations over the same frequency simultaneously through a shared AF relay, and closed-form approximation for the outage probability and an upper bound to the ergodic sum capacity are derived.

[22] proposes a self-energy recycling FD cooperative NOMA system, where a nearby user can be employed as a DF or AF relay with self-energy recycling protocol to assist a far user, and new expressions of exact and asymptotic outage probabilities for two users are derived. In [23], downlink cooperative multiple-input single-output wireless sensor networks with NOMA over Nakagami- $m$  fading are studied. Novel antenna-relay-destination selection schemes are proposed for DF and AF relaying strategies, and then, closed-form expressions of outage probability at the selected sensor nodes are derived. [24] investigates the performance of a virtual FD relaying technique in cooperative NOMA-based systems in which two HD AF relays imitate the operation of FD relaying, and the closed-form expression of outage probability is derived. In [25], a power-domain NOMA system with partial statistical channel state information (CSI) is studied and ergodic sum rate and outage probability are obtained for both DF and AF relaying strategies over Nakagami- $m$  fading channels. In [26], the authors obtained closed-form expressions of the outage probabilities for a two-stage relay selection strategy for DF and AF relaying protocols employed in NOMA networks where one base station (BS) communicates with two mobile users with the aid of multiple relays. The outage performance of a cooperative NOMA-based network that applies AF relaying protocol is studied in [27], and approximate outage probability and its asymptotic behaviors are obtained. In [28], performance of the fixed-gain AF relaying with NOMA is investigated over Nakagami- $m$  fading channels for two different scenarios where BS intends to communicate with multiple users through the assistance of AF relaying with and without LOS. A hybrid AF and DF with NOMA transmission scheme is proposed for a cellular system with multiple relays in [29]. It is shown that the proposed scheme can achieve larger sum channel capacity and larger average system throughput compared with the traditional schemes.

Furthermore, different system models for NOMA-enabled vehicular communication infrastructures are investigated throughout several works in the literature [30]–[35]. In [30], the exact expression of the average achievable rate of a NOMA-based cooperative relaying system over Rician fading channels is obtained. Outage probability expressions are derived for near and far user nodes whether they are on the roads (vehicle, cyclist, pedestrian) or outside the roads (BS, road side unit) in [31]. The secrecy outage probability performance of a NOMA-based vehicular communication system is analyzed and closed-form analytical expressions for the FD/HD relaying protocols over Nakagami- $m$  fading channels are derived in [32]. The outage performance analysis of cooperative vehicular networks is made and the closed-form outage probability expressions are obtained in [33] when the MRC technique is applied at the relay. In [34], a novel cooperative transmission scheme employing a signal superposition technique is proposed and a closed-form expression for the link reliability of the proposed scheme is derived. It is shown that high communication reliability may be achieved with this technique since vehicle user equipments (VUEs) superpose other VUEs' signals and then re-transmit other users' V2V packets. [35] analyzes the security performance

of the FD-NOMA based V2V system from the physical layer perspective, and then derives analytical results of the ergodic secrecy capacity. In this study, the authors also propose a secrecy sum rate optimization scheme utilizing the instantaneous CSI. In [36], two half-duplex/full-duplex relay-assisted NOMA-based scheme is investigated to solve optimum power allocation problem among the users to improve the quality-of-service with the poor channel conditions over independent Rayleigh distributed channels. The BER and ergodic capacity performance of NOMA-SM scheme in V2V Massive MIMO system has been investigated in [37]. Moreover, in [37], power allocation optimization scheme is studied over a spatio-temporally correlated Rician channel.

It should be noted that the channel models in all the abovementioned studies were selected from among channel models valid for cellular communication systems, and NOMA-based cooperative V2V communication systems over cascaded fading channels have not been studied in the literature yet. Additionally, performance of non-cooperative vehicular systems with NOMA over cascaded fading channels is investigated in [38]–[40]. In [38], the overall outage probability of two user-assisted NOMA-based V2V systems is studied over double Rayleigh fading channels. Joint power allocation optimization and the probability of successful decoding for caching-aided 2-user NOMA-based system is investigated for double Nakagami- $m$  fading channels in [39]. In [40], a vehicle clustering method is proposed and maximum achievable rate between clusters is studied over double Rayleigh fading channels.

## B. Motivation and Contribution

In V2V communication systems, fading channels may be much more hostile due to reasons such as high velocities of user nodes, low antenna-heights, and mostly unavailable LOS between transmitter and receiver. Therefore, to achieve robust communication at high data rates over far distances, some performance enhancement methods must be considered in the system design. Additionally, it has been shown that the fading coefficients of vehicular channels may be modeled as the multiplication of a number of random variables, and several studies in the literature show that the double Rayleigh fading model can adequately model this type of channels [10]–[12], [38], [40]. Additionally, in order to avoid the mathematical complexity, some papers in the literature consider the fading effects at the V2V links as Rayleigh fading or other fading models which are better than Rayleigh fading [41]–[43]. On the other hand, in our proposed system, V2V channels are assigned to be subject to the double Rayleigh fading which is the most accurately fitting fading model for the considered environment. At this point, we emphasize that for the first time in the literature, we propose to exploit the benefits of NOMA and fixed-gain AF relayed cooperative communication techniques together for V2V systems, and then investigate the performance of the proposed system in terms of outage probability and ergodic capacity metrics. Hence the main contributions of this paper can be summarized as follows:

- For the first time in the literature, a power-domain downlink NOMA-enabled cooperative vehicular communica-

tion system employing fixed-gain AF relaying scheme is proposed to cope with the severe fading conditions over double Rayleigh fading channels.

- We examine the performance of the proposed system by deriving the exact analytical expressions of outage probabilities in closed-form for near and far users over double Rayleigh fading channels.
- We obtain closed-form analytical expressions of the ergodic capacity to provide more insight into the vehicular communication systems' performance over double Rayleigh fading channels.
- We present the analytic and numerical results with respect to different system parameters such as transmitting power, distance between nodes, and the power allocation metrics to evaluate the performance of the vehicular communication system.
- Finally, we compared the NOMA system performance with the traditional OMA technique considering the outage probability and ergodic capacity analyses.

The remainder of the manuscript is organized as follows: Section II details the proposed system and the channel model. Section III investigates the outage probabilities at the near and far users. In Section IV, ergodic capacity for both users and the overall system are examined. In Section V, analytic and numerical results are provided to evaluate the system's performance and to verify the analytic result via Monte-Carlo simulations. Section VI concludes the paper.

Throughout this paper,  $F_X(\cdot)$  and  $f_X(\cdot)$  denote the CDF and the PDF of a random variable  $X$ , respectively, while  $E[\cdot]$  symbolizes the expectation operator.

## II. SYSTEM MODEL

One of the major distinctions between vehicular and conventional cellular communication systems is the antenna elevation of the nodes. In the proposed system, all vehicle nodes are assumed to be equipped with the antennas at low elevations and to be in motion, which results in local scattering around the vehicles causing delay and attenuation for the received signal. In this study, we consider a vehicular communication system with power-domain downlink NOMA which consists of a BS, a relay (R) and two paired users, i.e.,  $U_1$  (strong user) and  $U_2$  (weak user), as illustrated in Fig. 1. As a realistic scenario for the V2V communications in urban areas in which the LOS between BS and the end-users may not be available most of the time due to the high buildings around the vehicles, R is used as an intermediate relaying node to help BS communicate with the users. We assume that all nodes have a single antenna and operate in HD mode. Further,  $h_r$ ,  $h_1$  and  $h_2$  are the fading coefficients of the wireless channels between BS–R, R– $U_1$ , and R– $U_2$ , respectively. Also the distances between BS–R, R– $U_1$ , and R– $U_2$  are denoting by  $d_{sr}$ ,  $d_1$ , and  $d_2$ , respectively, and they are normalized with respect to the total distance between BS– $U_2$ , which is  $d_{sr} + d_2$ . Since R,  $U_1$  and  $U_2$  are nodes moving at high speeds, it is assumed that the corresponding channel coefficients  $h_1$  and  $h_2$  are double Rayleigh distributed while the channel coefficient  $h_r$  for BS→R has Rayleigh distribution due to the

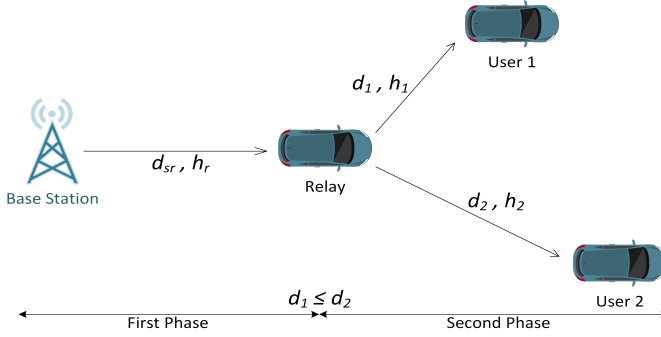


Fig. 1. NOMA-enabled cooperative vehicular communication system employing fixed-gain AF relaying.

fixed BS. Here,  $h_1$  and  $h_2$  can be expressed by a product of two single Rayleigh distributions, which in turn results in the envelope of the channel having a double Rayleigh fading distribution. Therefore, considering the double Rayleigh fading channel model, which is worse than the Rayleigh fading, for the vehicular communication systems is accurately reasonable. Furthermore, without loss of generality,  $d_1 \leq d_2$  and the channel gains of the users are ordered as  $|h_1|^2 \geq |h_2|^2$  and  $E[|h_i|^2] = \Omega_i$  for  $i \in \{1, 2\}$ .

In the system, information transmission occurs in two phases. During the first phase, BS broadcasts superimposed signals,  $s_1$  for  $U_1$  and  $s_2$  for  $U_2$ , to the node R with a total transmit power of  $P_t$ . Hence, the signal transmitted from the BS using the downlink NOMA technique is [44]

$$x = \sqrt{P_1}s_1 + \sqrt{P_2}s_2, \quad (1)$$

where  $P_1$  and  $P_2$  are the allocated powers for  $U_1$  and  $U_2$ , respectively, determined as  $P_1 = \alpha_1 P_t$  and  $P_2 = \alpha_2 P_t$ . Here  $\alpha_i$  is the power allocation coefficient and  $\alpha_1 + \alpha_2 = 1$ . By following the principle of NOMA, BS allocates more power to the weak user's signal than the strong user's signal so that  $\alpha_1 < \alpha_2$ . Hence, the signal received at R is

$$y_r = h_r x + n_r = h_r(\sqrt{P_1}s_1 + \sqrt{P_2}s_2) + n_r \quad (2)$$

where  $n_r \sim \mathcal{CN}(0, N_0)$  is the additive white Gaussian noise (AWGN) at R with power  $N_0$ . Then, in the second transmission phase, R applies the fixed-gain AF relaying technique and forwards the scaled signal to the users. Therefore, the signal received at the  $i^{\text{th}}$  user becomes

$$\begin{aligned} y_i &= Gh_i y_r + n_i \\ &= Gh_i h_r \underbrace{(\sqrt{P_1}s_1 + \sqrt{P_2}s_2)}_{\text{Signal broadcast from BS}} + \underbrace{Gh_i n_r + n_i}_{\text{Noise}} \end{aligned} \quad (3)$$

where  $G = \sqrt{\frac{P_r}{P_i \Omega_r + N_0}}$  is the power normalization factor and  $n_i \sim \mathcal{CN}(0, N_0)$  is the AWGN for the  $i^{\text{th}}$  user.

Due to the higher power level assigned to  $U_2$ 's symbols at BS, assuming perfect SIC is performed at the receiver,  $U_1$  first decodes  $s_2$  from the received signal  $y_1$ . Thus, the SINR related to the processing of  $s_2$  is given as

$$\gamma_{1,2} = \frac{G^2 |h_1|^2 |h_r|^2 P_2}{G^2 |h_1|^2 |h_r|^2 P_1 + G^2 |h_1|^2 N_0 + N_0}. \quad (4)$$

After successfully decoding  $s_2$ ,  $U_1$  subtracts the corresponding interference term from the received signal and obtains its own symbol  $s_1$  without any interference from the other user. Therefore, the obtained SNR corresponding to the decoding process of  $s_1$  becomes

$$\gamma_1 = \frac{G^2 |h_1|^2 |h_r|^2 P_1}{G^2 |h_1|^2 N_0 + N_0}. \quad (5)$$

In parallel, since  $s_1$  has been transmitted with a small portion of  $P_t$  from BS,  $U_2$  can decode its own symbol  $s_2$  directly from the received signal  $y_2$  without employing SIC by treating the corresponding term of  $s_1$  as interference. Hence the SINR achieved by  $U_2$  during the decoding process of  $s_2$  may be expressed as

$$\gamma_2 = \frac{G^2 |h_2|^2 |h_r|^2 P_2}{G^2 |h_2|^2 |h_r|^2 P_1 + G^2 |h_2|^2 N_0 + N_0}. \quad (6)$$

In the following sections, we investigate the performance of the proposed system in terms of outage probabilities and achievable ergodic capacities for both  $U_1$  and  $U_2$ .

### III. OUTAGE PROBABILITY ANALYSIS

#### A. Exact Outage Probability for the Near User

In the proposed system,  $U_1$  falls into outage regime when  $s_1$  or  $s_2$  cannot be decoded successfully by  $U_1$ . In other words, the outage regime might happen if  $\gamma_1$  or  $\gamma_{1,2}$  goes below a certain threshold value and can be probabilistically expressed as

$$P_{out}^1 = 1 - \mathcal{P}\{\gamma_{1,2} > \gamma_{th2}, \gamma_1 > \gamma_{th1}\} \quad (7)$$

where  $\gamma_{th1} = 2^{2\mathcal{R}_1} - 1$  and  $\gamma_{th2} = 2^{2\mathcal{R}_2} - 1$  are the predefined threshold values for  $U_1$  and  $U_2$ , respectively. Here,  $\mathcal{R}_1$  and  $\mathcal{R}_2$  are the targeted data rates at  $U_1$  and  $U_2$ , respectively. By substituting (4) and (5) into (7), the outage probability is obtained and simplified as

$$\begin{aligned} P_{out}^1 &= 1 - \mathcal{P}\left\{|h_r|^2 > \tau, |h_1|^2 > \left(\frac{\tau/G^2}{|h_r|^2 - \tau}\right)\right\} \\ &\times \mathcal{P}\left\{|h_r|^2 > \nu, |h_1|^2 > \left(\frac{\nu/G^2}{|h_r|^2 - \nu}\right)\right\} \end{aligned} \quad (8)$$

where  $\tau \triangleq \varrho_2 / (P_2 - P_1 \gamma_{th2})$ ,  $\nu \triangleq \varrho_1 / P_1$ ,  $\varrho_1 \triangleq N_0 \gamma_{th1}$  and  $\varrho_2 \triangleq N_0 \gamma_{th2}$ . Here, it is assumed that  $\gamma_{th2} < (P_2 / P_1)$ . Please note that, unless otherwise stated,  $P_{out}^1$  is always one. Then, by defining  $\phi \triangleq \max(\tau, \nu)$ , (8) is expressed in integral form as

$$\begin{aligned} P_{out}^1 &= 1 - \mathcal{P}\left\{|h_r|^2 > \phi, |h_1|^2 > \frac{\phi/G^2}{|h_r|^2 - \phi}\right\} \\ &= \int_0^\phi f_{|h_r|^2}(y) dy + \int_\phi^\infty f_{|h_r|^2}(y) F_{|h_1|^2}\left(\frac{\phi/G^2}{y - \phi}\right) dy. \end{aligned} \quad (9)$$

Since  $h_r$  is exposed to Rayleigh fading, the PDF of  $|h_r|^2$  is

$$f_{|h_r|^2}(\gamma) = \frac{1}{\bar{\gamma}_r} e^{-\frac{\gamma}{\bar{\gamma}_r}} \quad (10)$$

where  $\bar{\gamma}_r = \Omega_r$  [1]. Furthermore, for double Rayleigh fading channels, the CDF of the unordered channel gain  $|\tilde{h}|^2$  is [38]

$$F_{|\tilde{h}|^2}(\gamma) = 1 - 2\sqrt{\frac{\gamma}{\bar{\gamma}}} K_1 \left( 2\sqrt{\frac{\gamma}{\bar{\gamma}}} \right) \quad (11)$$

where  $K_v(\cdot)$  is the  $v^{\text{th}}$  order modified Bessel function of the second kind [45] and  $\bar{\gamma} = E[|\tilde{h}|^2]$ . Consequently, with the aid of order statistic [46], the CDF of the ordered channel gain in double Rayleigh fading channels becomes

$$F_{|h_l|^2}(\gamma) = \sum_{k=0}^{M-l} \frac{(-1)^k M!}{(l+k)(M-l-k)!(l-1)!k!} [F_{|\tilde{h}|^2}(\gamma)]^{l+k} \quad (12)$$

where  $M$  is the number of users and  $l$  is the order index. For the proposed system,  $M = 2$  and  $l = 2$ . Therefore, by substituting (11) in (12), CDF of the ordered channel gain  $|h_1|^2$  becomes

$$F_{|h_1|^2}(\gamma) = [F_{|\tilde{h}_1|^2}(\gamma)]^2 = 1 - \omega_1(\gamma, \bar{\gamma}_1) + \omega_2(\gamma, \bar{\gamma}_1) \quad (13)$$

where  $\bar{\gamma}_1 = \Omega_1$  while  $\omega_1(\cdot, \cdot)$  and  $\omega_2(\cdot, \cdot)$  are defined as

$$\omega_1(a, b) \triangleq 4\sqrt{\frac{a}{b}} K_1 \left( 2\sqrt{\frac{a}{b}} \right) \quad (14a)$$

and

$$\omega_2(a, b) \triangleq 4\frac{a}{b} \left[ K_1 \left( 2\sqrt{\frac{a}{b}} \right) \right]^2 \quad (14b)$$

where  $a$  is the parameter and  $b \in \{\bar{\gamma}_1, \bar{\gamma}_2\}$ , respectively. Thus, by using (10), (13), (14a) and (14b),  $P_{out}^1$  may be expressed as

$$P_{out}^1 = 1 - I_1 + I_2 \quad (15)$$

where

$$I_1 = \int_{\phi}^{\infty} f_{|h_r|^2}(\gamma) \omega_1 \left( \frac{\phi/G^2}{\gamma - \phi}, \bar{\gamma}_1 \right) d\gamma \quad (16)$$

and

$$I_2 = \int_{\phi}^{\infty} f_{|h_r|^2}(\gamma) \omega_2 \left( \frac{\phi/G^2}{\gamma - \phi}, \bar{\gamma}_1 \right) d\gamma. \quad (17)$$

Substituting (10) and the explicit expression of  $\omega_1$  in (16), and by applying  $\gamma - \phi = t$  transformation,  $I_1$  is becomes as

$$I_1 = 4\sqrt{\frac{\phi/G^2}{\bar{\gamma}_1}} \kappa_1 \int_0^{\infty} t^{-\frac{1}{2}} e^{-\frac{t}{\bar{\gamma}_r}} K_1 \left( 2\sqrt{\frac{1}{\bar{\gamma}_1} \frac{\phi/G^2}{t}} \right) dt \quad (18)$$

where  $\kappa_1 \triangleq \frac{1}{\bar{\gamma}_r} e^{-\frac{\phi}{\bar{\gamma}_r}}$ . After that, by using [47, 14], [45, 9.31-1], [45, 9.31-2], [45, 9.31-5] and [45, 7.813-1], the closed-form solution of (18) is obtained as

$$I_1 = 2e^{-\frac{\phi}{\bar{\gamma}_r}} G_{4,1}^{1,3} \left( \frac{\bar{\gamma}_1 \bar{\gamma}_r}{\phi/G^2} \middle| \begin{matrix} 0,0,1,-\frac{1}{2} \\ -\frac{1}{2} \end{matrix} \right) \quad (19)$$

where  $G_{p,q}^{m,n}(\cdot)$  denotes Meijer's G-function [45]. By substituting (10) and (14b) in (17), with the help of  $\gamma - \phi = t$  transformation and after some algebraic simplifications,  $I_2$  is written as

$$I_2 = \kappa_1 \int_0^{\infty} \frac{4\phi/G^2}{\bar{\gamma}_1 t} e^{-\frac{t}{\bar{\gamma}_r}} \left[ K_1 \left( 2\sqrt{\frac{1}{\bar{\gamma}_1} \frac{\phi/G^2}{t}} \right) \right]^2 dt. \quad (20)$$

Furthermore, first applying [47, 11] and [48, 03.04.26.0014.01] and then using [45, 9.31-5], [45, 9.31-1] and [45, 9.31-2], and finally with the help of [47, 21], (20) is solved and the closed-form solution for  $I_2$  is obtained as

$$I_2 = \frac{\sqrt{\pi}}{2} e^{-\frac{\phi}{\bar{\gamma}_r}} G_{6,3}^{2,4} \left( \frac{\bar{\gamma}_1 \bar{\gamma}_r}{4\phi/G^2} \middle| \begin{matrix} 0,1,-1,0,-1,-1 \\ -1,-1,-\frac{1}{2} \end{matrix} \right). \quad (21)$$

Finally, by substituting (19) and (21) in (15), the exact outage probability expression for the near user  $U_1$  is obtained in closed-form.

### B. Exact Outage Probability for the Far User

From the perspective of the far user, the outage regime occurs when  $U_2$  can not decode its own symbol  $s_2$  successfully due to receiving lower SNR value compared to the threshold value. As for its probability,  $P_{out}^2$  is given as

$$P_{out}^2 = \mathcal{P}\{\gamma_2 \leq \gamma_{th_2}\}. \quad (22)$$

By substituting (6) in (22),  $P_{out}^2$  takes the form

$$P_{out}^2 = \mathcal{P} \left\{ \frac{G^2 |h_2|^2 |h_r|^2 P_2}{G^2 |h_2|^2 |h_r|^2 P_1 + G^2 |h_2|^2 N_0 + N_0} \leq \gamma_{th_2} \right\} = \mathcal{P} \left\{ |h_2|^2 G^2 (|h_r|^2 \lambda - N_0 \gamma_{th_2}) \leq N_0 \gamma_{th_2} \right\} \quad (23)$$

where  $\lambda = P_2 - P_1 \gamma_{th_2}$ . From (23), it is seen that the outage probability at  $U_2$  can be written as

$$P_{out}^2 = \mathcal{P} \left\{ |h_r|^2 < \tau \right\} + \mathcal{P} \left\{ |h_r|^2 > \tau, |h_2|^2 < \frac{\tau/G^2}{|h_r|^2 - \tau} \right\}. \quad (24)$$

According to (24), the condition  $\gamma_{th_2} < P_2/P_1$  must be satisfied system-wide to keep the far user from being exposed to unavoidable outage condition. Further, by expressing (24) in integral form, it is written as

$$P_{out}^2 = \int_0^{\tau} f_{|h_r|^2}(y) dy + \int_{\tau}^{\infty} f_{|h_r|^2}(y) F_{|h_2|^2} \left( \frac{\tau/G^2}{|h_r|^2 - \tau} \right) dy. \quad (25)$$

By using (12) with  $M = 2$  and  $l = 1$  for  $U_2$ , the CDF of the ordered channel gain  $|h_2|^2$  for double Rayleigh fading channels is obtained as

$$F_{|h_2|^2}(\gamma) = 2F_{|\tilde{h}_2|^2}(\gamma) - [F_{|\tilde{h}_2|^2}(\gamma)]^2. \quad (26)$$

Then, by defining  $\chi \triangleq 2\sqrt{\frac{\gamma}{\bar{\gamma}_2}} K_1 \left( 2\sqrt{\frac{\gamma}{\bar{\gamma}_2}} \right)$  where  $\bar{\gamma}_2 = \Omega_2$  and substituting (11) in (26), (26) can be written as

$$F_{|h_2|^2}(\gamma) = 2(1 - \chi) - (1 - \chi)^2 = 1 - \chi^2 = 1 - \omega_2(\gamma, \bar{\gamma}_2) \quad (27)$$

Additionally, by substituting (27) into (25),  $P_{out}^2$  is written as

$$P_{out}^2 = 1 - I_3 \quad (28)$$

where

$$I_3 = \int_{\tau}^{\infty} f_{|h_r|^2}(\gamma) \omega_2 \left( \frac{\tau/G^2}{\gamma - \tau}, \bar{\gamma}_2 \right) d\gamma = \int_{\tau}^{\infty} \frac{4}{\bar{\gamma}_2} \frac{\tau/G^2}{\gamma - \tau} \left[ K_1 \left( 2\sqrt{\frac{1}{\bar{\gamma}_2} \frac{\tau/G^2}{\gamma - \tau}} \right) \right]^2 \frac{1}{\bar{\gamma}_r} e^{-\frac{\gamma}{\bar{\gamma}_r}} d\gamma \quad (29)$$

which is similar to the expression in (20) with the replacement of the parameter  $\phi$  with  $\tau$ . Therefore, by applying  $\gamma - \tau = t$  transformation and first applying [47, 11] and [48, 03.04.26.0014.01], then using [45, 9.31-5], [45, 9.31-1] and [45, 9.31-2], and finally with the help of [47, 21], (29) is solved and the closed-form solution for  $P_{out}^2$  is obtained as

$$P_{out}^2 = 1 - \frac{\sqrt{\pi}}{2} e^{-\frac{\tau}{\bar{\gamma}_r}} G_{5,2}^{1,4} \left( \frac{\bar{\gamma}_2 \bar{\gamma}_r}{4\tau/G^2} \middle| \begin{matrix} 0,0,1,-1,0 \\ 0,-\frac{1}{2} \end{matrix} \right). \quad (30)$$

### C. System Outage Probability

In this section, the overall system outage probability is defined as the probability of at least one user being exposed to outage through the system. Therefore, the overall outage probability of the considered system is calculated as

$$P_{out} = 1 - (1 - P_{out}^1)(1 - P_{out}^2) \quad (31)$$

where  $P_{out}^1$  and  $P_{out}^2$  are provided in (15) and (30), respectively.

## IV. ERGODIC CAPACITY ANALYSIS

In this section, the ergodic capacity analysis is presented, first for the near user  $U_1$  and then for the far user  $U_2$ .

### A. Ergodic Rate from BS to $U_1$

For the near user  $U_1$ , the ergodic capacity is given as [49]

$$\begin{aligned} R_{ave}^1 &= E \left[ \frac{1}{2} \log_2(1 + \gamma_1) \right] \\ &= \int_0^\infty \frac{1}{2} \log_2(1 + \gamma) f_{\gamma_1}(\gamma) d\gamma \\ &= \frac{1}{2 \ln 2} \int_0^\infty \frac{1 - F_{\gamma_1}(\gamma)}{1 + \gamma} d\gamma. \end{aligned} \quad (32)$$

By using (5),  $F_{\gamma_1}(\gamma)$  is calculated as

$$\begin{aligned} F_{\gamma_1}(\gamma) &= \mathcal{P} \left\{ \frac{G^2 |h_1|^2 |h_r|^2 P_1}{G^2 |h_1|^2 N_0 + N_0} < \gamma \right\} \\ &= \mathcal{P} \left\{ |h_1|^2 G^2 (|h_r|^2 P_1 - N_0 \gamma) < N_0 \gamma \right\}. \end{aligned} \quad (33)$$

From (33), it is observed that  $F_{\gamma_1}(\gamma)$  may be written as

$$\begin{aligned} F_{\gamma_1}(\gamma) &= \mathcal{P} \left\{ |h_r|^2 > \frac{N_0 \gamma}{P_1}, |h_1|^2 < \frac{N_0 \gamma / G^2}{|h_r|^2 P_1 - N_0 \gamma} \right\} \\ &+ \mathcal{P} \left\{ |h_r|^2 < \frac{N_0 \gamma}{P_1} \right\} \end{aligned} \quad (34)$$

which is expressed in integral form as

$$\begin{aligned} F_{\gamma_1}(\gamma) &= \int_{\frac{N_0 \gamma}{P_1}}^\infty f_{|h_r|^2}(h) F_{|h_1|^2} \left( \frac{N_0 \gamma / G^2}{h P_1 - N_0 \gamma} \right) dh \\ &+ \int_0^{\frac{N_0 \gamma}{P_1}} f_{|h_r|^2}(h) dh. \end{aligned} \quad (35)$$

Then, by substituting (13) in (35) and after some arrangements  $F_{\gamma_1}(\gamma)$  is written as,

$$F_{\gamma_1}(\gamma) = 1 - J_1 + J_2 \quad (36)$$

where

$$J_1 = \int_{\frac{N_0 \gamma}{P_1}}^\infty f_{|h_r|^2}(h) \omega_1 \left( \frac{N_0 \gamma / G^2}{h P_1 - N_0 \gamma}, \bar{\gamma}_1 \right) dh \quad (37)$$

while

$$J_2 = \int_{\frac{N_0 \gamma}{P_1}}^\infty f_{|h_r|^2}(h) \omega_2 \left( \frac{N_0 \gamma / G^2}{h P_1 - N_0 \gamma}, \bar{\gamma}_1 \right) dh. \quad (38)$$

Then, by using (10) and (14a), (37) becomes

$$\begin{aligned} J_1 &= \int_{\frac{N_0 \gamma}{P_1}}^\infty \frac{1}{\bar{\gamma}_r} e^{-\frac{h}{\bar{\gamma}_r}} 4 \sqrt{\frac{1}{\bar{\gamma}_1} \frac{N_0 \gamma / G^2}{h P_1 - N_0 \gamma}} \\ &\times K_1 \left( 4 \sqrt{\frac{1}{\bar{\gamma}_1} \frac{N_0 \gamma / G^2}{h P_1 - N_0 \gamma}} \right) dh. \end{aligned} \quad (39)$$

Applying  $t = h P_1 - N_0 \gamma$  transformation, (39) is written as

$$\begin{aligned} J_1 &= \kappa_2 \sqrt{\frac{N_0 \gamma / G^2}{\bar{\gamma}_1}} \\ &\times \int_0^\infty t^{-1/2} e^{-\frac{t}{\bar{\gamma}_r P_1}} K_1 \left( 2 \sqrt{\frac{1}{\bar{\gamma}_1} \frac{N_0 \gamma / G^2}{t}} \right) dt \end{aligned} \quad (40)$$

where  $\kappa_2 = \frac{4}{\bar{\gamma}_r P_1} e^{-\frac{N_0 \gamma}{\bar{\gamma}_r P_1}}$ . After that, by using [47, 11] and [45, 9.31-1,2,4,5], [47, 14] and [45, 9.31-2] and [45, 9.31-5], (40) is solved as

$$J_1 = 2e^{-\frac{N_0 \gamma}{\bar{\gamma}_r P_1}} G_{2,5}^{3,2} \left( \frac{N_0 \gamma / G^2}{\bar{\gamma}_r \bar{\gamma}_1 P_1} \middle| \begin{matrix} 2, \frac{3}{2} \\ 1, 1, 0, \frac{3}{2}, 2 \end{matrix} \right). \quad (41)$$

Furthermore, by substituting (10) and (14b) in (38) and using  $t = h P_1 - N_0 \gamma$  transformation,  $J_2$  is expressed as

$$\begin{aligned} J_2 &= \kappa_2 \frac{N_0 \gamma / G^2}{\bar{\gamma}_1} \\ &\times \int_0^\infty t^{-1} e^{-\frac{t}{\bar{\gamma}_r P_1}} \left[ K_1 \left( 2 \sqrt{\frac{1}{\bar{\gamma}_1} \frac{N_0 \gamma / G^2}{t}} \right) \right]^2 dt. \end{aligned} \quad (42)$$

Then, applying [48, 03.04.26.0014.01], [45, 9.31-5], [45, 9.31-1], [45, 9.31-2] and [45, 7.813-1] respectively,  $J_2$  is derived as

$$J_2 = \frac{\sqrt{\pi}}{2} e^{-\frac{N_0 \gamma}{\bar{\gamma}_r P_1}} G_{5,2}^{1,4} \left( \frac{\bar{\gamma}_1 \bar{\gamma}_r P_1}{4 N_0 \gamma / G^2} \middle| \begin{matrix} 0,0,1,-1,0 \\ 0,-\frac{1}{2} \end{matrix} \right). \quad (43)$$

Besides, by using (41) and (43) in (32), the ergodic capacity for the near user  $U_1$  is calculated as

$$R_{ave}^1 = \frac{1}{2 \ln 2} \int_0^\infty \frac{J_1 - J_2}{1 + \gamma} d\gamma = \frac{1}{2 \ln 2} [\mathcal{M}_1 - \mathcal{M}_2] \quad (44)$$

where

$$\mathcal{M}_1 = 2 \int_0^\infty \frac{e^{-\frac{N_0 \gamma}{\bar{\gamma}_r P_1}}}{1 + \gamma} G_{2,5}^{3,2} \left( \frac{N_0 \gamma / G^2}{\bar{\gamma}_r \bar{\gamma}_1 P_1} \middle| \begin{matrix} 2, \frac{3}{2} \\ 1, 1, 0, \frac{3}{2}, 2 \end{matrix} \right) d\gamma, \quad (45)$$

and

$$\mathcal{M}_2 = \frac{\sqrt{\pi}}{2} \int_0^\infty \frac{e^{-\frac{N_0 \gamma}{\bar{\gamma}_r P_1}}}{1 + \gamma} G_{5,2}^{1,4} \left( \frac{\bar{\gamma}_1 \bar{\gamma}_r P_1}{4 N_0 \gamma / G^2} \middle| \begin{matrix} 0,0,1,-1,0 \\ 0,-\frac{1}{2} \end{matrix} \right) d\gamma. \quad (46)$$

Using Meijer's G representations of polynomial and exponential functions as  $(1+x)^\alpha = \frac{1}{\Gamma(-\alpha)} G_{1,1}^{1,1} \left( x \middle| \begin{smallmatrix} 1+\alpha \\ 0 \end{smallmatrix} \right)$  [47, 10] and  $e^{-x} = G_{0,1}^{1,0} \left( x \middle| \begin{smallmatrix} - \\ 0 \end{smallmatrix} \right)$  [47, 11], (45) can be expressed as

$$\mathcal{M}_1 = 2 \int_0^\infty G_{1,1}^{1,1} \left( \gamma \middle| \begin{smallmatrix} 0 \\ 0 \end{smallmatrix} \right) G_{0,1}^{1,0} \left( \frac{N_0 \gamma}{\bar{\gamma}_r P_1} \middle| \begin{smallmatrix} - \\ 0 \end{smallmatrix} \right) \times G_{2,5}^{3,2} \left( \frac{N_0 \gamma / G^2}{\bar{\gamma}_r \bar{\gamma}_1 P_1} \middle| \begin{smallmatrix} 2, \frac{3}{2} \\ 1, 1, 0, \frac{3}{2}, 2 \end{smallmatrix} \right) d\gamma \quad (47)$$

and with the help of [48, 07.34.21.0081.01],  $\mathcal{M}_1$  is obtained as

$$\mathcal{M}_1 = 2G_{1,1:0,1:2,5}^{1,1:1,0:3,2} \left( \frac{N_0}{\bar{\gamma}_r P_1}, \frac{N_0 / G^2}{\bar{\gamma}_r \bar{\gamma}_1 P_1} \middle| \begin{smallmatrix} 0 \\ 0 \end{smallmatrix} \middle| \begin{smallmatrix} 2, \frac{3}{2} \\ 1, 1, 0, \frac{3}{2}, 2 \end{smallmatrix} \right) \quad (48)$$

in closed-form where  $G_{p,q:p_1,q_1:p_2,q_2}^{m,n:m_1,n_1:m_2,n_2} (\cdot, \cdot, \cdot, \cdot, \cdot, \cdot)$  is the extended generalized bi-variate Meijer's G function [50]. It should be noted that the well-known numeric computing environments have not yet included the bi-variate Meijer's G as a built-in function, but several algorithms for its calculation are available in the literature [51].

Further, by following similar steps,  $\mathcal{M}_2$  is written as

$$\mathcal{M}_2 = \frac{\sqrt{\pi}}{2} \int_0^\infty G_{1,1}^{1,1} \left( \gamma \middle| \begin{smallmatrix} 0 \\ 0 \end{smallmatrix} \right) G_{0,1}^{1,0} \left( \frac{N_0 \gamma}{\bar{\gamma}_r P_1} \middle| \begin{smallmatrix} - \\ 0 \end{smallmatrix} \right) \times G_{5,2}^{1,4} \left( \frac{\bar{\gamma}_1 \bar{\gamma}_r P_1}{4N_0 \gamma / G^2} \middle| \begin{smallmatrix} 0, 0, 1, -1, 0 \\ 0, -\frac{1}{2} \end{smallmatrix} \right) d\gamma \quad (49)$$

and using [48, 07.34.21.0081.01], it is derived as

$$\mathcal{M}_2 = \frac{\sqrt{\pi}}{2} G_{1,1:0,1:2,5}^{1,1:1,0:4,1} \left( \frac{N_0}{\bar{\gamma}_r P_1}, \frac{4N_0 / G^2}{\bar{\gamma}_r \bar{\gamma}_1 P_1} \middle| \begin{smallmatrix} 0 \\ 0 \end{smallmatrix} \middle| \begin{smallmatrix} 1, \frac{3}{2} \\ 1, 1, 0, 2, 1 \end{smallmatrix} \right) \quad (50)$$

in closed-form. Finally, by substituting (48) and (50) in (44), the ergodic capacity expression for the near user  $U_1$  can be obtained in closed-form.

### B. Ergodic Rate from BS to $U_2$

By following steps similar to those in finding out  $R_{ave}^1$ , the ergodic capacity for  $U_2$  is written as

$$R_{ave}^2 = E \left[ \frac{1}{2} \log_2 (1 + \gamma_2) \right] = \frac{1}{2 \ln 2} \int_0^\infty \frac{1 - F_{\gamma_2}(\gamma)}{1 + \gamma} d\gamma \quad (51)$$

where  $F_{\gamma_2}(\gamma)$  is expressed as follows, with the help of (6),

$$F_{\gamma_2}(\gamma) = \mathcal{P} \left\{ \frac{G^2 |h_2|^2 |h_r|^2 P_2}{G^2 |h_2|^2 |h_r|^2 P_1 + G^2 |h_2|^2 N_0 + N_0} < \gamma \right\} = \mathcal{P} \left\{ |h_r|^2 > \frac{N_0 \gamma}{P_2 - P_1 \gamma}, |h_2|^2 < \frac{N_0 \gamma / G^2}{|h_r|^2 (P_2 - P_1 \gamma) - N_0 \gamma} \right\} + \mathcal{P} \left\{ |h_r|^2 < \frac{N_0 \gamma}{P_2 - P_1 \gamma} \right\} \quad (52)$$

and from the requirement  $\gamma < P_2 / P_1$ , (52) becomes

$$F_{\gamma_2}(\gamma) = \int_0^{\frac{N_0 \gamma}{\beta}} f_{|h_r|^2}(h) dh + \int_{\frac{N_0 \gamma}{\beta}}^\infty f_{|h_r|^2}(h) F_{|h_2|^2} \left( \frac{N_0 \gamma / G^2}{h \beta - N_0 \gamma} \right) dh \quad (53)$$

where  $\beta = P_2 - P_1 \gamma$ . Then, by using the CDF of the ordered channel gain for  $U_2$ , given by (27), (53) takes the form

$$F_{\gamma_2}(\gamma) = 1 - J_3 \quad (54)$$

where  $J_3$  is

$$J_3 = \int_{\frac{N_0 \gamma}{\beta}}^\infty f_{|h_r|^2}(h) \omega_2 \left( \frac{N_0 \gamma / G^2}{\beta h - N_0 \gamma}, \bar{\gamma}_2 \right) dh. \quad (55)$$

Thus,  $R_{ave}^2$  is written as

$$R_{ave}^2 = \frac{1}{2 \ln 2} \int_0^{\frac{P_2}{P_1}} \frac{J_3}{1 + \gamma} d\gamma. \quad (56)$$

It is worth pointing out that  $J_3$  has an integral expression similar to  $J_2$  with the replacement of the parameters  $\bar{\gamma}_1$  with  $\bar{\gamma}_2$ , and  $P_1$  with  $\beta$  in (38). Therefore, by following steps similar to those in deriving  $J_2$ ,  $J_3$  is obtained as

$$J_3 = J_2 \Big|_{\bar{\gamma}_1 \rightarrow \bar{\gamma}_2, P_1 \rightarrow \beta} = \frac{\sqrt{\pi}}{2} e^{-\frac{N_0 \gamma}{\bar{\gamma}_r \beta}} G_{5,2}^{1,4} \left( \frac{\bar{\gamma}_2 \bar{\gamma}_r \beta}{4N_0 \gamma / G^2} \middle| \begin{smallmatrix} 0, 0, 1, -1, 0 \\ 0, -\frac{1}{2} \end{smallmatrix} \right). \quad (57)$$

Finally, by substituting (57) in (56), the ergodic capacity at the far user is obtained as

$$R_{ave}^2 = \frac{1}{2 \ln 2} \frac{\sqrt{\pi}}{2} \int_0^{\frac{P_2}{P_1}} \frac{1}{1 + \gamma} e^{-\frac{N_0 \gamma}{\bar{\gamma}_r \beta}} \times G_{5,2}^{1,4} \left( \frac{\bar{\gamma}_2 \bar{\gamma}_r \beta}{4N_0 \gamma / G^2} \middle| \begin{smallmatrix} 0, 0, 1, -1, 0 \\ 0, -\frac{1}{2} \end{smallmatrix} \right) d\gamma. \quad (58)$$

Please note that the single integral form in (58) is not analytically tractable. Therefore, it should be evaluated numerically.

### C. Overall Ergodic Rate

For the proposed system, the overall achievable ergodic capacity is calculated as

$$R_{ave} = R_{ave}^1 + R_{ave}^2. \quad (59)$$

where  $R_{ave}^1$  and  $R_{ave}^2$  are provided in (44) and (58), respectively.

## V. NUMERICAL RESULTS AND SIMULATIONS

In this section, the performance of the proposed NOMA-enabled cooperative V2V system is presented through numerical calculations of the analytic derivations by comparing simulations for miscellaneous scenarios. During the calculations and Monte-Carlo trials, it is assumed that all nodes, BS, R,  $U_1$ , and  $U_2$ , align on a straight line and the noise variance at each node is set to  $N_0 = 1$ . Without loss of generality, the average channel gains are considered to be associated with the corresponding distances between the nodes as  $\Omega_{sr} = 1/(1 + d_{sr}^2)$ ,  $\Omega_1 = 1/(1 + d_1^2)$  and  $\Omega_2 = 1/(1 + d_2^2)$ . Additionally, the obtained results of the proposed system are compared with the simulation results of the traditional cooperative OMA (COMA) technique [52] to provide better and comprehensive insight into the performance of the NOMA technique. Herein, the received SNRs of using COMA technique considering (3) are calculated as  $\gamma_i^{COMA} =$

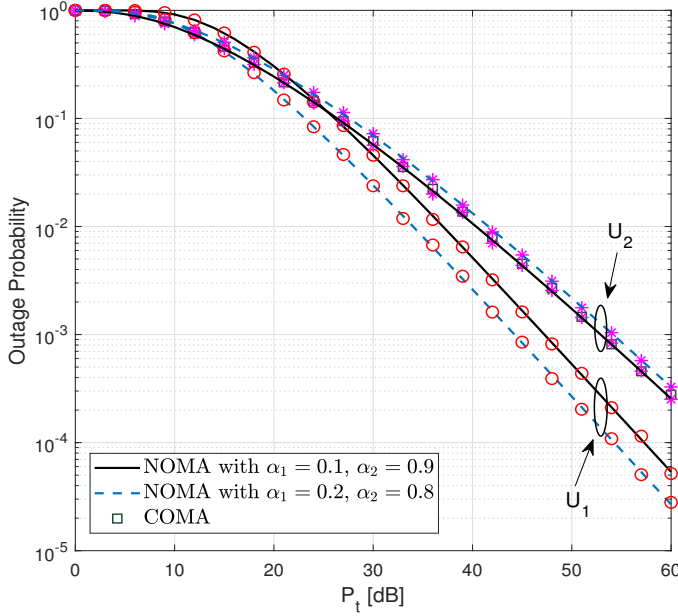


Fig. 2. The outage performance of the near and far users in the proposed NOMA-enabled vehicular communication system and comparison with the COMA.  $\mathcal{R}_1 = \mathcal{R}_2 = 0.5$  bit/Hz/s and  $(d_{sr}, d_1, d_2) = (0.5, 0.5, 0.5)$ .

$G|h_i|^2|h_r|^2P_t/(G|h_i|^2N_0 + N_0)$  and the corresponding rate is given as  $\mathcal{R}_i^{COMA} = 0.25 \log_2(1 + \gamma_i^{COMA})$  where  $i \in \{1, 2\}$  for the near and far users, respectively. Please note that, the rate of applying the COMA technique is half the rate of using the NOMA technique since the symbol of users are not transmitted simultaneously in the COMA scheme [2]. Moreover, for a fair comparison between COMA and NOMA, we assume that each user is allocated equal bandwidth and equal transmission power. Furthermore, the presented figures show the analytical and Monte-Carlo simulation results together to verify the derivations, where the markers on the plots represent simulation outcomes while the lines show numerical results of the analytic expressions.

Fig. 2 shows the variation of the outage probabilities for both users with respect to the total transmitting power  $P_t$  for two different power allocation regimes at the BS,  $\alpha_1 = 0.1$  ( $\alpha_2 = 0.9$ ) and  $\alpha_1 = 0.2$  ( $\alpha_2 = 0.8$ ). Here, the simulation results of the COMA scheme are also provided for the sake of comparison. In the proposed system, since the symbol transmission from BS to the users takes two time slots and by assuming that BS uses the same modulation scheme for both users, let us say a binary modulation scheme, target data rates are assigned as  $\mathcal{R}_1 = \mathcal{R}_2 = 0.5$  bit/Hz/s. Further, the normalized distances are chosen as  $d_{sr} = 0.5$ ,  $d_1 = 0.5$  and  $d_2 = 0.5$ . The figure shows that increasing the power ratio  $\alpha_1$  from 0.1 to 0.2, which means doubling the transmission power allocated to  $U_1$  (i.e., 100% increase), provides 3 dB SNR gain for the outage performance of  $U_1$  with the strong channel. On the other hand, decreasing the power ratio  $\alpha_2$  from 0.9 to 0.8, which means 11.5% reduction at the transmission power allocated to  $U_2$ , results in an approximately 1.5 dB SNR loss at the outage probability performance of  $U_2$  with

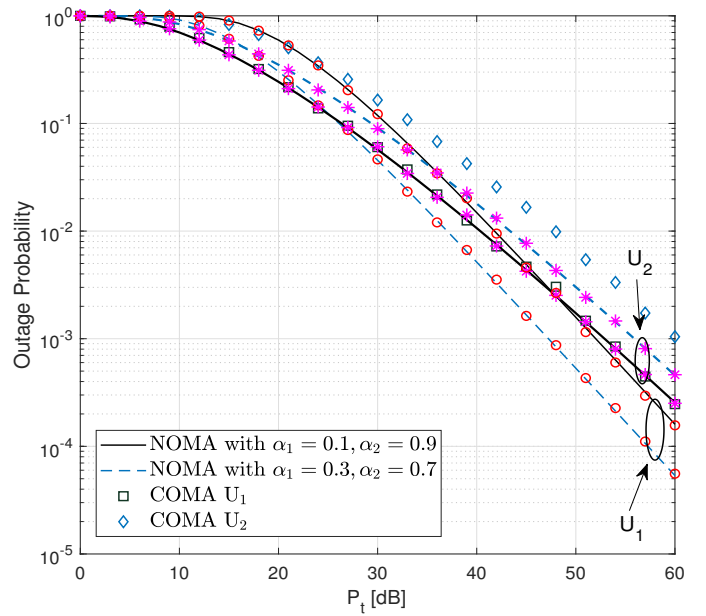


Fig. 3. The outage performance comparison of NOMA and COMA techniques over double Rayleigh fading channels.  $\mathcal{R}_1 = 1$  bit/Hz/s,  $\mathcal{R}_2 = 0.5$  bit/Hz/s and  $(d_{sr}, d_1, d_2) = (0.5, 0.5, 0.5)$ .

the weak channel. This tells us that the effective gain of  $U_1$  becomes greater than the effective loss of  $U_2$  as the  $P_2/P_1$  ratio decreases and therefore overall system performance can also be enhanced in this way. Furthermore, Fig. 2 presents the performance of the COMA scheme and it reveals that the outage performance of the NOMA scheme at  $U_1$  outperforms the COMA's since the channel gain of  $U_1$  is greater than that of  $U_2$ . On the other hand, it is shown that the performance of COMA for  $U_2$  becomes slightly better with the increasing  $\alpha_1$  value. However, it is worth noting that the NOMA scheme will offer better spectral efficiency and user fairness than COMA as multiple users are operated simultaneously.

The outage probability performances of  $U_1$  and  $U_2$  with respect to the total transmitting power  $P_t$  are depicted in comparison with the COMA scheme in Fig. 3. Here the target data rates are chosen as  $\mathcal{R}_1 = 1$  bit/Hz/s and  $\mathcal{R}_2 = 0.5$  bit/Hz/s while the distances are assumed to be  $d_{sr} = 0.5$ ,  $d_1 = 0.5$  and  $d_2 = 0.5$ . Comparing the performance plot of  $U_1$  in Fig. 2 for  $\alpha_1 = 0.1$  and  $\mathcal{R}_1 = 0.5$  bit/Hz/s with that in Fig. 3 for  $\alpha_1 = 0.3$  and  $\mathcal{R}_1 = 1$  bit/Hz/s, it is observed that  $U_1$  has similar outage performance, for example  $9 \times 10^{-3}$  and  $6 \times 10^{-3}$  at 50 dB. Therefore, by allocating more power,  $U_1$  can double its target data rate with a negligible loss in the outage performance. On the other hand, as expected, the outage performance of  $U_2$  gets worse with increasing  $\alpha_1$ . Furthermore, it is seen from the figure that the performance of  $U_2$  surpasses  $U_1$  for  $\alpha_1 = 0.1$  at low and middle SNR regions due to the substantially low transmit power of the BS for  $U_1$  when  $P_t < 45$  dB. The figure also shows that the outage performance of  $U_1$  with COMA technique is better than the NOMA-enabled transmitting scheme when  $\alpha_1 = 0.1$  for SNR values up to 45 dB. This is due to the fact that since the

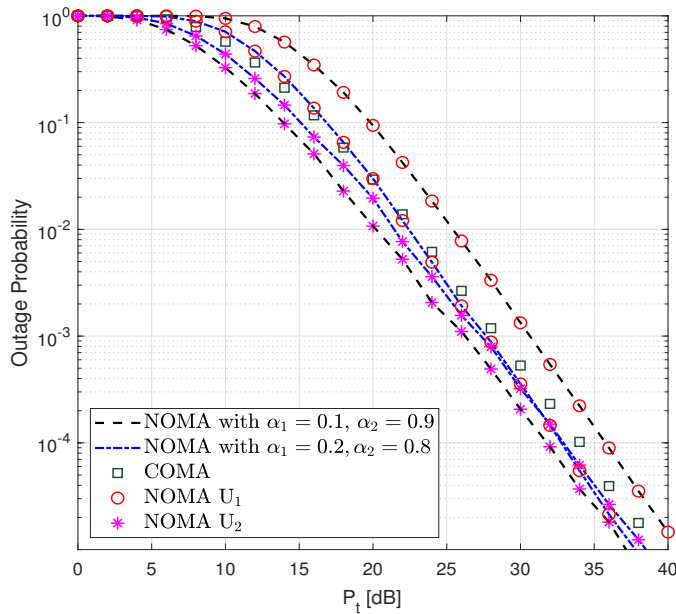


Fig. 4. The outage performance of the near and far users for using Nakagami- $m$  fading for all channels in NOMA-enabled vehicular communication system.  $(d_{sr}, d_1, d_2) = (0.5, 0.5, 0.5)$ ,  $m = 2$  and  $\mathcal{R}_1 = \mathcal{R}_2 = 0.5$  bit/Hz/s

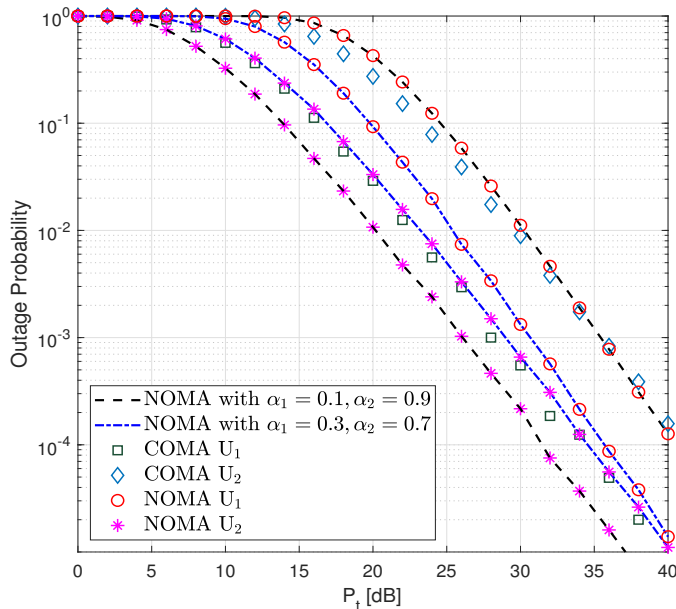


Fig. 5. The outage performance of the near and far users for using Nakagami- $m$  fading for all channels in NOMA-enabled vehicular communication system.  $(d_{sr}, d_1, d_2) = (0.5, 0.5, 0.5)$ ,  $m = 2$ ,  $\mathcal{R}_1 = 1$  bit/Hz/s and  $\mathcal{R}_2 = 0.5$  bit/Hz/s

rate of  $U_1$  in COMA is half of the NOMA and more power is allocated to  $U_1$  in COMA, outage probability outperforms compared to NOMA at low SNR. Besides, NOMA shows better performance for  $U_1$  at high SNR when  $\alpha_1 = 0.1$  since its performance is exponentially increased by the increasing transmit power of the BS considering (5). However, it is obvious that the NOMA technique will provide better spectral

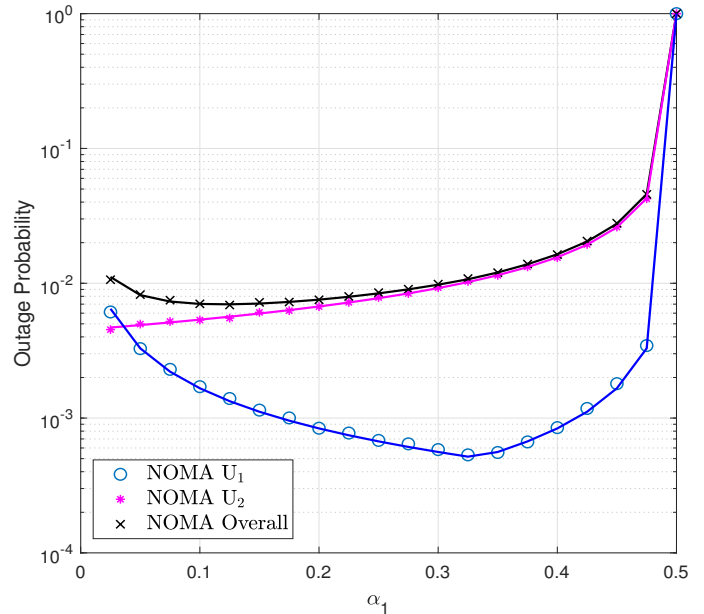


Fig. 6. The outage probability performances of the overall system and the users in the NOMA-enabled cooperative vehicular communication system.  $\mathcal{R}_1 = \mathcal{R}_2 = 0.5$  bit/Hz/s,  $(d_{sr}, d_1, d_2) = (0.5, 0.5, 0.8)$  and  $P_t = 45$  dB.

efficiency than the COMA method since two users are assisted simultaneously in the proposed system.

Fig. 4 presents the performance of the proposed system using the same system parameters in Fig. 2 over Nakagami- $m$  fading channels to provide a comparison with the double Rayleigh fading channels. For a fair comparison, we set the Nakagami- $m$  parameter of both channels to the same value as  $m = 2$ . Since the fading conditions in Nakagami- $m$  channels are better than those in the double Rayleigh channels, power allocation among the users affects their performances that yields the performance of  $U_2$  becomes better than  $U_1$ 's performance. It is seen from Fig. 2 that, an increase in  $\alpha_1$  from 0.1 to 0.2 results in an enhancement in the  $U_1$ 's system performance while the system performance of  $U_2$  degrades. Moreover, when considering the Nakagami- $m$  fading channels, system performance of both users act as similar as in the case of the double Rayleigh fading channels. Furthermore, it is seen from Fig. 4 that the approximately 26 dB SNR gain is achieved for the outage probability of  $10^{-3}$  when assuming the Nakagami- $m$  fading channels for COMA.

Fig. 5 shows the variation of the outage probability with  $P_t$  in the proposed system where the channels are subject to Nakagami- $m$  fading, instead of the double Rayleigh fading. Here again, the Nakagami- $m$  parameter values for both channels are assigned the same as  $m = 2$ . Apart from Fig. 3, it is seen from Fig. 5 that  $U_2$  outperforms  $U_1$  in terms of system performance, since more power is allocated for  $U_2$ . Contrary to the observed results in Fig. 3, the increasing  $\alpha_1$  causes the increasing outage probability for  $U_1$  while  $U_2$ 's outage probability decreases. Furthermore, when employing COMA scheme over Nakagami- $m$  fading channels, approximately 25 dB SNR gain for  $U_1$  and  $U_2$  is achieved to have the outage

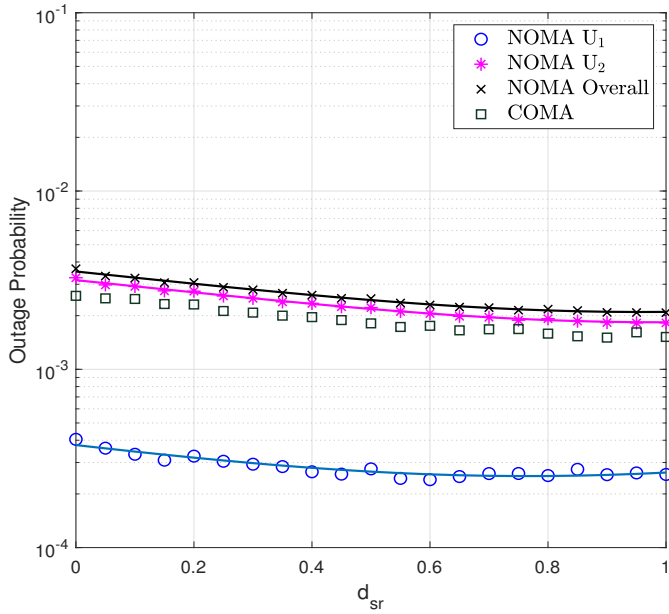


Fig. 7. The outage performance comparison of NOMA and COMA techniques with respect to the distance between BS and the relay.  $(\alpha_1, \alpha_2) = (0.2, 0.8)$ ,  $\mathcal{R}_1 = 0.5$  bit/Hz/s,  $\mathcal{R}_2 = 0.5$  bit/Hz/s, and  $P_t = 50$  dB.

probability of  $10^{-3}$  when comparing with the double Rayleigh fading channels.

The outage probability performances of both users and the overall system performance with respect to the power allocation parameter  $\alpha_1$  is presented in Fig. 6. Here,  $P_t = 45$  dB and the normalized distances are  $d_{sr} = d_1 = 0.5$  and  $d_2 = 0.8$ . The figure shows that the outage probability performance of the overall system and  $U_2$  converge to each other in the range  $0.32 \leq \alpha_1 < 0.5$ . It is also seen that  $\alpha_1 = 0.32$  value, which is the starting point for the convergence of the outage probabilities for  $U_2$  and the overall system, is the optimum power allocation coefficient value for  $U_1$ . The figure also reveals that increasing the allocated power for  $U_1$  causes degradation in the power level of  $U_2$ , since  $U_1$ 's performance also degrades due to the SIC procedure failure. Further, it can be observed that for  $\alpha_1 > 0.5$ , the criteria  $\gamma_{th2} < P_2/P_1$  in (8) cannot be satisfied and the outage probabilities rapidly reach 1.

Fig. 7 depicts the outage probabilities of  $U_1$ ,  $U_2$  and the overall system versus distance  $d_{sr}$ . Here, the system parameters are set to  $P_t = 50$  dB,  $\alpha_1 = 0.2$  ( $\alpha_2 = 0.8$ ),  $\mathcal{R}_1 = 0.5$  bit/Hz/s, and  $\mathcal{R}_2 = 0.5$  bit/Hz/s. Furthermore, the distances between BS- $U_1$  and BS- $U_2$  are assigned as  $d = 1$ . However, R is in motion under the assumption  $d_1 = d_2 = d - d_{sr}$ . From the figure, it is observed that  $U_1$  has a better performance compared to  $U_2$ , since the channel gain of  $U_1$  is greater than that of  $U_2$ . Therefore, NOMA outperforms COMA for the strong user  $U_1$ . On the other hand, as an important result, it is seen that COMA has slightly better outage performance than NOMA for the weak user  $U_2$ . However, NOMA still has the advantages of providing better spectral efficiency and user fairness as multiple users use the same frequency band at the

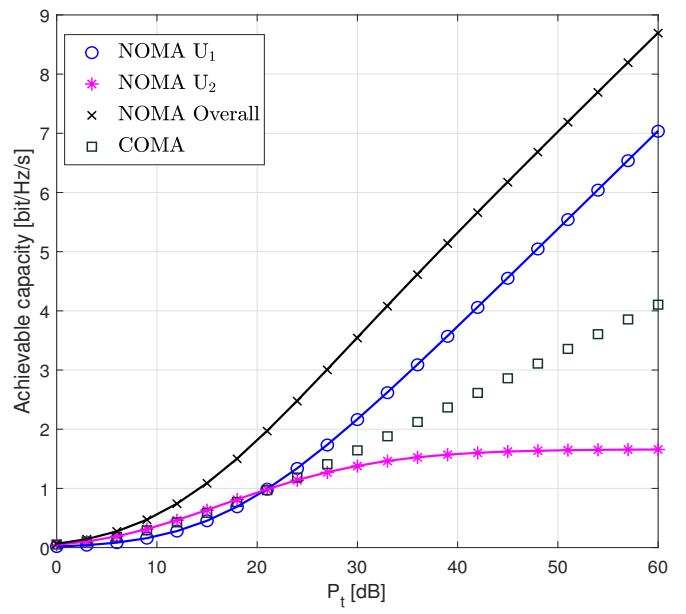


Fig. 8. The comparison of ergodic capacity of the users and the overall system for COMA and NOMA for  $(d_{sr}, d_1, d_2) = (0.5, 0.5, 0.5)$  where for NOMA  $(\alpha_1, \alpha_2) = (0.1, 0.9)$ .

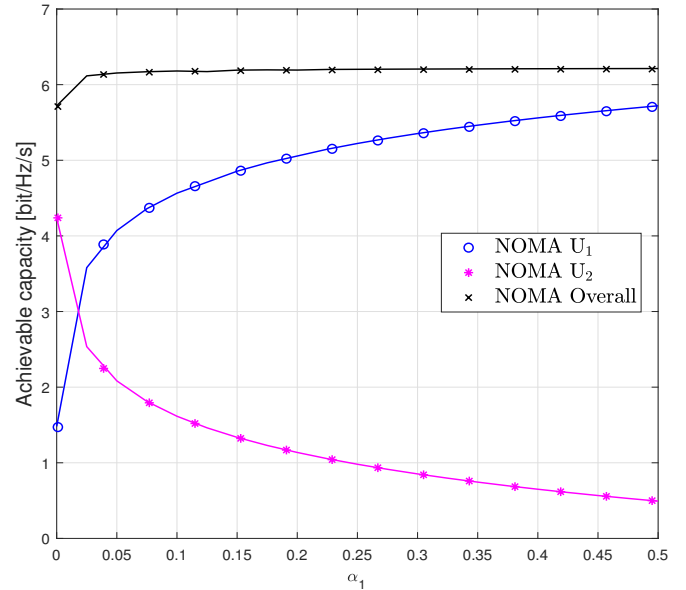


Fig. 9. The ergodic capacities of the near and far users and of the overall system.  $P_t = 45$  dB and  $(d_{sr}, d_1, d_2) = (0.5, 0.5, 0.8)$ .

same time.

For the proposed system, achievable ergodic capacity for the overall system and also the ergodic capacities for  $U_1$  and  $U_2$  are presented in Fig. 8 for NOMA and COMA schemes, with respect to  $P_t$  for the case of  $\alpha_1 = 0.1$  ( $\alpha_2 = 0.9$ ). The figure reveals that increasing  $P_t$  results in saturation at the achievable rate performance of  $U_2$  at high SNR due to interference from  $U_1$ . However, since  $U_1$  is able to perfectly

decode its information without an interference from  $U_2$  after a successful SIC operation, its own and therefore the overall system performance increase. It is also shown that  $U_1$  reaches higher achievable capacity values when using NOMA technique compared to the case of employing traditional COMA scheme while the achievable capacity for  $U_2$  for COMA technique is better than that for the NOMA method.

Finally, the ergodic capacity performances of the proposed system is given in Fig. 9 for changing  $\alpha_1$  values when  $P_t = 45$  dB and the normalized distances are assigned as  $d_{sr} = 0.5$ ,  $d_1 = 0.5$  and  $d_2 = 0.8$ . The figure shows that the overall achievable data rate saturates to approximately 6 bit/Hz/s even for small values of  $\alpha_1$  while increasing  $\alpha_1$  provides higher achievable data rates for  $U_1$ . However, the achievable data rate for  $U_2$  decreases in this case.

## VI. CONCLUSION

In this paper, performance of the NOMA-enabled cooperative vehicular communication systems, where the transmission from the base station to the end-users has been established with the help of a relay employing fixed-gain AF relaying scheme has been investigated. Since the fading channels in vehicular communication systems exhibit cascaded fading characteristics, theoretical analyses have been carried out by considering the double Rayleigh fading channel model as a realistic fading scheme. Moreover, the results are compared with the Nakagami- $m$  fading. During the analyses, we first obtained closed-form expressions for the outage probabilities of the strong/near and weak/far users; after that, the exact ergodic capacities for these users have been derived under double Rayleigh fading. Then we provided the numerical results of the calculations of analytic expressions for different system parameters and verified them by Monte-Carlo simulations. We also provided the simulation results for the COMA scheme and compared the performances of NOMA and COMA methods in the proposed V2V communication system. The results show that the near user has better performance in the NOMA-enabled systems compared to the systems employing the COMA technique due to the SIC being perfectly applied on the near user. On the other hand, the performance of the weak user worsens in case of using the NOMA technique compared to the COMA method even though the allocated power at the base station for the near user remains at small values.

## ACKNOWLEDGMENT

The work of Semiha Koşu was supported by the Research Fund of the Istanbul Technical University under Project MYL-2019-42491.

## REFERENCES

- [1] M. Simon and M. Alouini, *Digital Communication over Fading Channels*. Wiley, 2005.
- [2] Y. Saito, Y. Kishiyama, A. Benjebbour, T. Nakamura, A. Li, and K. Higuchi, "Non-orthogonal Multiple Access (NOMA) for Cellular Future Radio Access," in *Proc. IEEE Veh. Tech. Conf.*, 2013, pp. 1–5.
- [3] S. A. A. Shah, E. Ahmed, M. Imran, and S. Zeadally, "5G for Vehicular Communications," *IEEE Commun. Magazine*, vol. 56, no. 1, pp. 111–117, 2018.
- [4] Y. Yang and K. Hua, "Emerging Technologies for 5G-Enabled Vehicular Networks," *IEEE Access*, vol. 7, pp. 181–117, 2019.
- [5] G. Luo, Q. Yuan, H. Zhou, N. Cheng, Z. Liu, F. Yang, and X. S. Shen, "Cooperative Vehicular Content Distribution in Edge Computing Assisted 5G-VANET," *China Commun.*, vol. 15, no. 7, pp. 1–17, 2018.
- [6] J. Lee and B. Park, "Development and Evaluation of a Cooperative Vehicle Intersection Control Algorithm Under the Connected Vehicles Environment," *IEEE Trans. on Intelligent Transportation Systems*, vol. 13, no. 1, pp. 81–90, 2012.
- [7] S. K. Gehrig and F. J. Stein, "Collision Avoidance for Vehicle-Following Systems," *IEEE Trans. on Intelligent Transportation Systems*, vol. 8, no. 2, pp. 233–244, 2007.
- [8] S. Darbha, S. Konduri, and P. R. Pagilla, "Benefits of V2V Communication for Autonomous and Connected Vehicles," *IEEE Trans. on Intelligent Transportation Systems*, vol. 20, no. 5, pp. 1954–1963, 2019.
- [9] Y. Ibdah and Y. Ding, "Statistical properties for Cascaded Rayleigh Fading Channel Models," in *Proc. 9th Int. Conf. on Inf., Commun. Signal Process.*, 2013, pp. 1–5.
- [10] V. Erceg, S. J. Fortune, J. Ling, A. J. Rustako, and R. A. Valenzuela, "Comparisons of a Computer-based Propagation Prediction Tool with Experimental Data Collected in Urban Microcellular Environments," *IEEE Journal on Selected Areas in Commun.*, vol. 15, no. 4, pp. 677–684, 1997.
- [11] D. W. Matolak and J. Frolik, "Worse-than-Rayleigh fading: Experimental Results and Theoretical Models," *IEEE Commun. Magazine*, vol. 49, no. 4, pp. 140–146, 2011.
- [12] V. Erceg, S. Fortune, J. Ling, A. Rustako, and R. Valenzuela, "Comparisons of a computer-based propagation prediction tool with experimental data collected in urban microcellular environments," *IEEE Journal on Selected Areas in Communications*, vol. 15, no. 4, pp. 677–684, 1997.
- [13] M. Seyfi, S. Muhaidat, J. Liang, and M. Uysal, "Relay Selection in Dual-Hop Vehicular Networks," *IEEE Signal Process. Lett.*, vol. 18, no. 2, pp. 134–137, Feb. 2011.
- [14] D. Qin, Y. Wang, and T. Zhou, "Performance Analysis of Bidirectional AF Based Cooperative Vehicular Networks," *IEEE Trans. on Veh. Tech.*, vol. 69, no. 2, pp. 2274–2279, Feb. 2020.
- [15] Y. Alghorani, G. Kaddoum, S. Muhaidat, and S. Pierre, "On the Approximate Analysis of Energy Detection Over  $n^*$  Rayleigh Fading Channels Through Cooperative Spectrum Sensing," *IEEE Wireless Commun. Lett.*, vol. 4, no. 4, pp. 413–416, Aug. 2015.
- [16] A. Al Hammadi, O. Alhussain, P. C. Sofotasios, S. Muhaidat, M. Al-Qutayri, S. Al-Araji, G. K. Karagiannidis, and J. Liang, "Unified Analysis of Cooperative Spectrum Sensing Over Composite and Generalized Fading Channels," *IEEE Trans. on Veh. Tech.*, vol. 65, no. 9, pp. 6949–6961, Sep. 2016.
- [17] P. S. Bithas, G. P. Efthymoglou, and A. G. Kanatas, "V2V Cooperative Relaying Communications Under Interference and Outdated CSI," *IEEE Trans. on Veh. Tech.*, vol. 67, no. 4, pp. 3466–3480, April 2018.
- [18] S. Wang, D. Wang, C. Li, and W. Xu, "Full Duplex AF and DF Relaying Under Channel Estimation Errors for V2V Communications," *IEEE Access*, vol. 6, pp. 65 321–65 332, 2018.
- [19] O. Abbasi, A. Ebrahimi, and N. Mokari, "NOMA Inspired Cooperative Relaying System Using an AF Relay," *IEEE Wireless Commun. Lett.*, vol. 8, no. 1, pp. 261–264, Feb. 2019.
- [20] M. Tian, S. Zhao, Q. Li, and J. Qin, "Secrecy Sum Rate Optimization in Nonorthogonal Multiple Access AF Relay Networks," *IEEE Systems Journal*, vol. 13, no. 3, pp. 2712–2715, Sep. 2019.
- [21] Y. Li, Y. Li, Y. Chen, Y. Ye, and H. Zhang, "Performance Analysis of Cooperative NOMA with a Shared AF Relay," *IET Commun.*, vol. 12, no. 19, pp. 2438–2447, 2018.
- [22] Z. Wang, X. Yue, and Z. Peng, "Full-Duplex User Relaying for NOMA System With Self-Energy Recycling," *IEEE Access*, vol. 6, pp. 67 057–67 069, 2018.
- [23] D. Tran, D. Ha, V. N. Vo, C. So-In, H. Tran, T. G. Nguyen, Z. A. Baig, and S. Sanguanpong, "Performance Analysis of DF/AF Cooperative MISO Wireless Sensor Networks With NOMA and SWIPT Over Nakagami- $m$  Fading," *IEEE Access*, vol. 6, pp. 56 142–56 161, 2018.
- [24] Q. Y. Liau, C. Y. Leow, and Z. Ding, "Amplify-and-Forward Virtual Full-Duplex Relaying-Based Cooperative NOMA," *IEEE Wireless Commun. Lett.*, vol. 7, no. 3, pp. 464–467, June 2018.
- [25] D. Wan, M. Wen, F. Ji, Y. Liu, and Y. Huang, "Cooperative NOMA Systems With Partial Channel State Information Over Nakagami- $m$  Fading Channels," *IEEE Trans. on Commun.*, vol. 66, no. 3, pp. 947–958, March 2018.
- [26] Z. Yang, Z. Ding, Y. Wu, and P. Fan, "Novel Relay Selection Strategies for Cooperative NOMA," *IEEE Trans. on Veh. Tech.*, vol. 66, no. 11, pp. 10 114–10 123, Nov. 2017.

- [27] X. Liang, Y. Wu, D. W. K. Ng, Y. Zuo, S. Jin, and H. Zhu, "Outage Performance for Cooperative NOMA Transmission with an AF Relay," *IEEE Commun. Lett.*, vol. 21, no. 11, pp. 2428–2431, Nov. 2017.
- [28] X. Yue, Y. Liu, S. Kang, and A. Nallanathan, "Performance Analysis of NOMA With Fixed Gain Relaying Over Nakagami- $m$  Fading Channels," *IEEE Access*, vol. 5, pp. 5445–5454, 2017.
- [29] Y. Liu, G. Pan, H. Zhang, and M. Song, "Hybrid Decode-Forward Amplify-Forward Relaying With Non-Orthogonal Multiple Access," *IEEE Access*, vol. 4, pp. 4912–4921, 2016.
- [30] R. Jiao, L. Dai, J. Zhang, R. MacKenzie, and M. Hao, "On the Performance of NOMA-Based Cooperative Relaying Systems Over Rician Fading Channels," *IEEE Trans. on Veh. Tech.*, vol. 66, no. 12, pp. 11409–11413, Dec. 2017.
- [31] B. E. Y. Belmekki, A. Hamza, and B. Escrig, "On the Outage Probability of Cooperative 5G NOMA at Intersections," in *Proc. IEEE 89th Veh. Tech. Conf. (VTC2019-Spring)*, April 2019, pp. 1–6.
- [32] W. Xie, J. Liao, C. Yu, P. Zhu, and X. Liu, "Physical Layer Security Performance Analysis of the FD-Based NOMA-VC System," *IEEE Access*, vol. 7, pp. 115568–115573, 2019.
- [33] B. E. Y. Belmekki, A. Hamza, and B. Escrig, "Outage Analysis of Cooperative NOMA Using Maximum Ratio Combining at Intersections," in *Proc. Int. Conf. on Wireless and Mobile Computing, Net. and Commun. (WiMob)*, Oct. 2019, pp. 1–6.
- [34] T. Kim, Y. Park, H. Kim, and D. Hong, "Cooperative Superposed Transmission in Cellular-Based V2V Systems," *IEEE Trans. on Veh. Tech.*, vol. 68, no. 12, pp. 11888–11901, Dec. 2019.
- [35] L. Wei, Y. Chen, D. Zheng, and B. Jiao, "Secure Performance Analysis and Optimization for FD-NOMA Vehicular Communications," *China Commun.*, vol. 17, no. 11, pp. 29–41, Nov. 2020.
- [36] G. Liu, Z. Wang, J. Hu, Z. Ding, and P. Fan, "Cooperative noma broadcasting/multicasting for low-latency and high-reliability 5g cellular v2x communications," *IEEE Internet of Things Journal*, vol. 6, no. 5, pp. 7828–7838, 2019.
- [37] Y. Chen, L. Wang, Y. Ai, B. Jiao, and L. Hanzo, "Performance analysis of noma-sm in vehicle-to-vehicle massive mimo channels," *IEEE Journal on Selected Areas in Communications*, vol. 35, no. 12, pp. 2653–2666, 2017.
- [38] N. Jaiswal and N. Purohit, "Performance Evaluation of Non-orthogonal Multiple Access in V2V communications Over Double-Rayleigh Fading Channels," in *Proc. IEEE Conf. on Inf. and Commun. Tech.*, Dec. 2019, pp. 1–5.
- [39] S. Gurugopinath, P. C. Sofotasios, Y. Al-Hammadi, and S. Muhaidat, "Cache-Aided Non-Orthogonal Multiple Access for 5G-Enabled Vehicular Networks," *IEEE Trans. on Veh. Tech.*, vol. 68, no. 9, pp. 8359–8371, Sep. 2019.
- [40] H. Xiao, Y. Chen, S. Ouyang, and A. T. Chronopoulos, "Power Control for Clustering Car-Following V2X Communication System With Non-Orthogonal Multiple Access," *IEEE Access*, vol. 7, pp. 68160–68171, 2019.
- [41] A. Pandey and S. Yadav, "Joint impact of nodes mobility and imperfect channel estimates on the secrecy performance of cognitive radio vehicular networks over nakagami-m fading channels," *IEEE Open Journal of Vehicular Technology*, vol. 2, pp. 289–309, 2021.
- [42] Y. Cui, G. Nie, and H. Tian, "Hop progress analysis of two-layer vanets with variant transmission range," *IEEE Wireless Communications Letters*, vol. 8, no. 5, pp. 1473–1476, 2019.
- [43] K. Koufos and C. P. Dettmann, "Outage in motorway multi-lane vanets with hardcore headway distance using synthetic traces," *IEEE Transactions on Mobile Computing*, vol. 20, pp. 2445–2456, 2021.
- [44] J. Men and J. Ge, "Performance Analysis of Non-orthogonal Multiple Access in Downlink Cooperative Network," *IET Commun.*, vol. 9, no. 18, pp. 2267–2273, 2015.
- [45] I. S. Gradshteyn and I. M. Ryzhik, *Table of Integrals, Series, and Products*. 7th edition, MA, USA: Elsevier, 2007.
- [46] H. A. David and H. N. Nagaraja, *Order Statistics*. NJ, USA: John Wiley & Sons, Inc., 2003.
- [47] V. S. Adamchik and O. I. Marichev, "The Algorithm for Calculating Integrals of Hypergeometric Type Functions and Its Realization in REDUCE System," in *Proc. Int. Symp. on Symbolic and Algebraic Comput.*, ser. ISSAC '90, 1990, pp. 212–224.
- [48] Wolfram Inc., "The mathematical functions site," <http://functions.wolfram.com>, 2018, [Online].
- [49] J. Men, J. Ge, and C. Zhang, "Performance Analysis of Nonorthogonal Multiple Access for Relaying Networks over Nakagami- $m$  Fading Channels," *IEEE Trans. on Veh. Tech.*, vol. 66, no. 2, pp. 1200–1208, 2017.
- [50] S. C. Gupta, "Integrals Involving Products of G-function," in *Proc. Indian Academy of Sciences - Section A*, 1969, p. 193–200.
- [51] H. Chergui, M. Benjillali, and S. Saoudi, "Performance Analysis of Project-and-Forward Relaying in Mixed MIMO-Pinhole and Rayleigh Dual-Hop Channel," *IEEE Commun. Lett.*, vol. 20, no. 3, pp. 610–613, March 2016.
- [52] Q. Zhang, K. Luo, W. Wang, and T. Jiang, "Joint c-oma and c-noma wireless backhaul scheduling in heterogeneous ultra dense networks," *IEEE Transactions on Wireless Communications*, vol. 19, no. 2, pp. 874–887, Feb 2020.



**Semiha Koşu** received the B.S. degree from Anadolu University, Eskisehir, Turkey, in 2018 and the M.Sc. degree in Satellite Communication and Remote Sensing Program from Informatics Institute, Istanbul Technical University, Istanbul, in 2021. She is currently a research assistant and working toward a Ph.D. degree with the Department of Information and Communication Engineering, Istanbul Technical University, Istanbul, Turkey. Her current research interests include the performance analysis of vehicular communications, cooperative communications, and non-orthogonal multiple access techniques.



**Serdar Özgür Ata** received the B.Sc., M.Sc., and Ph.D. degrees all in electronics and telecommunication engineering from Istanbul Technical University (ITU), Istanbul, Turkey, in 1996, 2010, and 2017, respectively. He has been chief researcher at the Scientific and Technological Research Council of Turkey - Informatics and Information Security Research Center (TÜBİTAK-BİLGEM) since 2002. He has been working as project manager in several secure voice and data communication projects. He also continues his academic studies in collaboration with Information and Communications Research Group in ITU Informatics Institute. His current research interests are in wireless communications including space-time coding, physical layer network coding, physical layer security, mobile-to-mobile/vehicle-to-vehicle communications and free space optical communications.